

Transport of charged particles propagating in turbulent magnetic fields as a red-noise processOLIVIER DELIGNY¹¹*Laboratoire de Physique des 2 Infinis Irène Joliot-Curie
CNRS/IN2P3, Université Paris-Saclay, Orsay, France*

Submitted to ApJ

ABSTRACT

The transport of charged particles in various astrophysical environments permeated by magnetic fields is described in terms of a diffusion process, which relies on diffusion-tensor parameters generally inferred from Monte-Carlo simulations. In this paper, a theoretical derivation of the diffusion coefficient in the case of a purely turbulent magnetic field is presented. The approach is based on a red-noise approximation to model the 2-pt correlation function of the magnetic field experienced by the particles between two successive times. This approach is shown to describe the regime in which the Larmor radius of the particles is in resonance with the wavelength power spectrum of the turbulence (gyro-resonant regime), extending hence previous results applying to the high-rigidity regime in which the Larmor radius is greater than the larger wavelength of the turbulence. The results are shown to be consistent with those obtained with a Monte-Carlo generator. Although not considered in this study, the presence of a mean field on top of the turbulence is discussed.

Keywords: cosmic rays — diffusion — magnetic fields — turbulence

1. INTRODUCTION

Many astrophysical environments such as jets, galaxies, clusters of galaxies, and interplanetary, interstellar or intergalactic space are considered as collisionless turbulent plasmas for the propagation and acceleration of high-energy charged particles (cosmic rays), the confinement and transport of which are governed by their scattering off magnetic turbulence. This is because the fluctuating magnetic field permeating these environments acts as an effective source of collisions in the transport equation of the velocity distribution of the particles (Jokipii 1972). Once approximated as a relaxation process, the effective collision term tends to bring the average velocity distribution to its isotropic mean (Bhatnagar et al. 1954). It is then well established that the flux of particles can be related to their gradient of density by means of a diffusion tensor D_{ij} , which can be expressed in terms of the magnetic field unit vector \mathbf{b} , the diffusion coefficients parallel and perpendicular to the mean field D_{\parallel} and D_{\perp} , and the anti-symmetric diffusion coefficient D_A describing the parti-

cle drifts as (Jones 1990)

$$D_{ij} = D_{\perp} \delta_{ij} + (D_{\parallel} - D_{\perp}) b_i b_j + D_A \epsilon_{ijk} b_k. \quad (1)$$

As long as the fluctuating field $\delta\mathbf{B}$ is subdominant with respect to the regular field \mathbf{B} , the level of turbulence defined as $\eta = \delta B^2 / (\delta B^2 + B^2)$ is low and the diffusion coefficients can be determined using a quasi-linear theory approach (Jokipii 1966, 1973). However, there are many situations of interest for which the turbulence level is found to be of the order of 0.5 (turbulent field of the order of the regular field) or even close to 1 (pure turbulent field). In such turbulence level regimes, many estimates of the diffusion coefficients have been made from numerical simulations exploring wide ranges of particle rigidities (e.g. Giacalone & Jokipii 1999; Casse et al. 2001; Candia & Roulet 2004; Hauff et al. 2010; Fatuzzo & Melia 2014; Snodin et al. 2016; Reichherzer et al. 2020, 2021).

In the high rigidity regime, which is relevant in situations where the Larmor radius of the particles exceeds the coherence length of the turbulence, a theoretical derivation of the coefficients, in agreement with the numerical results, has been formulated in Plotnikov et al. (2011). It is based on the exact estimation of the average

velocity of the particles propagating in the turbulence as a function of time, which is expressed as a Dyson series. In this regime, the values of the magnetic field experienced by the particles decorrelate on time scales much smaller than that of the scattering. This allows the use of a white-noise model for the 2-pt function of the magnetic field experienced between two successive times. Under these conditions, the re-summation of the Dyson series gives rise to an exponential decay of the average velocity characteristic of a Markovian process.

The aim of this study is to extend the results presented in Plotnikov et al. (2011) to a range of rigidities gyro-resonant with the power spectrum of turbulence. Although the methods employed can be applied to any type of turbulence, this paper is limited, without loss of generalities, to the study of an isotropic 3D turbulence without helicity. The general properties of such a 3D turbulence are reminded in Section 2, as well as the numerical and formal methods based on a Dyson series to determine the time evolution of the mean particle velocities and the 2-pt velocity functions. The red-noise assumption to model the 2-pt function of the magnetic field experienced between two successive times, which allows the introduction of a short time memory, is presented in Section 3. It is then shown that this assumption, which makes possible a partial re-summation of the Dyson series, allows the numerical results to be reproduced at the cost, just as in the white-noise case, of a single time parameter related to the turbulence correlation time. From these methods, the diffusion coefficients, which reduced to a single one in the $\eta = 1$ studied case, are reproduced in both the gyro-resonant and high-energy regimes. The presence of a mean field on top of a turbulence is discussed in Section 4, where some theoretical hints are given. The results are finally discussed in Section 5.

2. TRANSPORT OF CHARGED PARTICLES IN ISOTROPIC MAGNETIC TURBULENCE

2.1. Diffusion of charged particles in magnetic turbulence

For a random motion, the spatial diffusion tensor is known to be related under very broad conditions to the velocity correlation function, $\langle v_{0i} v_j(t) \rangle$, through a time integration (Kubo 1957),

$$D_{ij}(t) = \int_0^t dt' \langle v_{0i} v_j(t') \rangle, \quad (2)$$

in the limit that $t \rightarrow \infty$. Here, $v_{0i} \equiv v_i(t=0)$ and $\langle \cdot \rangle$ stands for the average quantities, taken over several space and time correlation scales of the turbulent field. Throughout the paper, since cosmic rays are high-energy

relativistic particles, the norm of the velocity is identified to c for convenience. The fluctuations are considered as ergodic, in the sense that averaging over an ensemble of systems would lead to the same average quantities as through the operation $\langle \cdot \rangle$. The aim of the study is hence to determine a semi-analytical expression for the velocity correlation function. The fluctuating magnetic field, denoted as $\delta \mathbf{B}(\mathbf{x})$ in the spatial space and $\delta \mathbf{B}(\mathbf{k})$ in the reciprocal Fourier one, is characterized in a standard way as a Gaussian random field with zero mean and root mean square value δB^2 modeling a 3D homogeneous and isotropic turbulence without helicity. For an homogeneous turbulence, the 2-pt correlation function between two components of $\delta \mathbf{B}(\mathbf{x})$ is invariant under spatial translations. In the Fourier space, this translates into

$$\langle \delta B_i(\mathbf{k}) \delta B_j^*(\mathbf{k}') \rangle = P_{ij}(\mathbf{k}) \delta(\mathbf{k} - \mathbf{k}'), \quad (3)$$

which states that two Fourier components of the field are uncorrelated at different wave-number vectors. The P_{ij} quantity is the spectral tensor defined as the Fourier transform of the 2-pt correlation function. To guarantee the solenoidal nature of the field, the spectral tensor must satisfy $k_i P_{ij} = k_j P_{ij} = 0$, a condition which, combined with the 3D isotropic character of the turbulence imposing rotational invariance on the 2-pt correlation function and with the invariance by symmetry with respect to a plane (no helicity of the field), implies the form $P_{ij}(\mathbf{k}) = \beta(k)(\delta_{ij} - k_i k_j / k^2)$ (Batchelor 1970), with $\beta(k)$ any function at this stage. On inserting this expression into the kinetic energy spectrum of the turbulence defined as

$$\mathcal{E}(k) = \frac{1}{2} \int_{\Sigma_k} d\Sigma P_{ii}(\mathbf{k}), \quad (4)$$

with Σ_k standing for the sphere of radius k in the Fourier space, one is left with the relationship $\mathcal{E}(k) = 4\pi k^2 \beta(k)$ so that the spectral tensor can finally be expressed as a function of a directly interpretable quantity:

$$P_{ij}(\mathbf{k}) = \frac{\mathcal{E}(k)}{4\pi k^2} \left(\delta_{ij} - \frac{k_i k_j}{k^2} \right). \quad (5)$$

The size of the largest “eddies”, L_{\max} , is given by the distance over which the correlation function is non-zero. This translates into a minimum wave number $k_{\min} = 2\pi/L_{\max}$ beyond which, for the Kolmogorov turbulence adopted here, the spectrum function follows a power law, $\mathcal{E}(k) = \mathcal{E}_0 k^{-5/3}$, up to a maximum wave number $k_{\max} = 2\pi/L_{\min}$, where L_{\min} corresponds to the scale at which the dissipation rate of the turbulence overcomes the energy cascade rate. The normalisation \mathcal{E}_0 is such that $\langle |\delta \mathbf{B}(\mathbf{x})|^2 \rangle = \delta B^2$:

$$\mathcal{E}_0 = \frac{(2\pi)^{2/3} \delta B^2}{3 \left(L_{\max}^{2/3} - L_{\min}^{2/3} \right)}. \quad (6)$$

There are several ways to characterize the distance L_c over which the correlation function of the turbulence is non-zero in the real space. We follow here that of Plotnikov et al. (2011),

$$L_c = \int_0^\infty dr \frac{\langle \delta B_i(\mathbf{x}) \delta B_i(\mathbf{x} + \mathbf{r}) \rangle}{\delta B^2}, \quad (7)$$

which leads, for the Kolmogorov turbulence, to $L_c = (L_{\max}^{5/3} - L_{\min}^{5/3}) / [10(L_{\max}^{2/3} - L_{\min}^{2/3})]$. This is a quantity of interest to estimate in Section 3.1, the correlation time that provides the duration beyond which a particle experiences a field value decorrelated from the initial one.

2.2. Monte-Carlo approach

To serve as a reference for testing the model below, a Monte-Carlo estimation of the velocity correlation function is used. The strategy of this Monte-Carlo experiment is similar to that widely used in the literature. A large number of particle trajectories in given turbulent magnetic field configurations is simulated by solving numerically the Lorentz-Newton equation of motion that preserves the energy (and hence the Lorentz factor) of the particles:

$$\dot{v}_i(t) = \delta\Omega \epsilon_{ijk} v_j(t) \delta b_k(t). \quad (8)$$

Here, $\delta\Omega = c^2 Z |e| \delta B / E$ is the gyrofrequency with $Z|e|$ the electric charge and E the energy of the particle, and $\delta b_k(t) \equiv \delta b_k(\mathbf{x}(t))$ is the k -th component of the magnetic field, expressed in units of δB , at the spatial coordinate $\mathbf{x}(t)$ of the particle at time t . The numerical integration of equation 8 is performed using the standard Runge-Kutta integrator. To approximate numerically the isotropic and spatially homogeneous turbulent field, an algorithm similar to that in Batchelor (1970); Giacalone & Jokipii (1999) is used. The recipe consists in summing a large number N_m of plane waves ($N_m = 250$ in this study) with corresponding wave vector \mathbf{k}_n , the direction, phase ϕ_n and polarisation of which are chosen randomly:

$$\delta \mathbf{B}(\mathbf{x}) = \sum_{n=1}^{N_m} \sum_{\alpha=1}^2 \mathcal{E}_n(k_n) \hat{\xi}_n^\alpha \cos(\mathbf{k}_n \cdot \mathbf{x} + \phi_n^\alpha). \quad (9)$$

To ensure the condition $\nabla \cdot \delta \mathbf{B} = 0$, the two orthogonal polarisation vectors $\hat{\xi}_n^\alpha$ are oriented in the plane perpendicular to the directions of the wave vectors. The wave number distribution is built from a constant logarithmic spacing between k_{\min} and k_{\max} . The wave amplitudes satisfy $\mathcal{E}_n^2(k_n) = \mathcal{E}_0 \delta B^2 k_n^{-5/3} (k_n - k_{n-1})$, where \mathcal{E}_0 is a normalisation factor such that $\sum_n \mathcal{E}_n^2(k_n) = \delta B^2$. The dynamic range of the turbulence explored here is $L_{\max}/L_{\min} = 100$.

2.3. Formal approach: Dyson series

Due to the stochastic nature of the magnetic field, the velocity of the particles is a stochastic variable as well, the probability density function of which can be sampled by means of the Monte-Carlo generator described in Section 2.2. Formally, the moments of this underlying distribution can be obtained by expressing the solution of equation 8 as a Dyson series. The first moment reads as

$$\begin{aligned} \langle v_{i_0}(t) \rangle &= v_{0i_0} + \sum_{n=1}^{\infty} \delta\Omega^n \epsilon_{i_0 i_1 j_1} \epsilon_{i_1 i_2 j_2} \dots \epsilon_{i_{n-1} i_n j_n} v_{0i_n} \\ &\times \int_0^t dt_1 \int_0^{t_1} dt_2 \dots \int_0^{t_{n-1}} dt_n \langle \delta b_{j_1}(t_1) \dots \delta b_{j_n}(t_n) \rangle \end{aligned} \quad (10)$$

which requires evaluating the expectation value in the integrand of the right-hand side. In the Gaussian approximation, the Wick theorem allows for expressing this expectation value in terms of all possible permutations of products of contractions of pairs of $\langle \delta b_{i_1}(t_{j_1}) \delta b_{i_2}(t_{j_2}) \rangle$. Using the Ansatz

$$\langle \delta b_{i_1}(t_{j_1}) \delta b_{i_2}(t_{j_2}) \rangle = \frac{\delta_{i_1 i_2}}{3} \varphi(t_{j_1} - t_{j_2}), \quad (11)$$

and making use of the summation properties over one or two indexes of the Levi-Civita symbol, the first moment of the velocities can be expressed as $\langle v_i(t) \rangle = u(t) v_{0i}$, where the “propagator” $u(t)$ reads as

$$\begin{aligned} u(t) &= 1 + \sum_{n=1}^{\infty} \left(\frac{-2\delta\Omega^2}{3} \right)^n \\ &\times \int_0^t dt_1 \int_0^{t_1} dt_2 \dots \int_0^{t_{2n-1}} dt_{2n} \sum_{\{i < j\}} \prod \varphi(t_i - t_j). \end{aligned} \quad (12)$$

Here, the notation $\sum_{\{i < j\}} \prod \varphi(t_i - t_j)$ stands for the $(2n-1)!!$ permutations of products of contractions of pairs.

In the following, it will be useful to represent the various terms of the expansion of $u(t)$ in the form of diagrams. The function $u(t)$ is considered as a propagator denoted by a double line, while a single line stands for the corresponding “free propagator”, $u^{(0)}(t) = 1$, which can be inserted in between the contraction of a pair, $\langle b_{i_1}(t_{j_1}) \delta b_{i_2}(t_{j_2}) \rangle = \langle \delta b_{i_1}(t_{j_1}) u^{(0)}(t) \delta b_{i_2}(t_{j_2}) \rangle$, to build an “interaction”. A curved dotted line connecting two “vertices” then stands for a time-ordered integration over an average product of two stochastic fields:

$$\text{---}\overbrace{\hspace{1cm}}^{\text{---}}\text{---} = \left(\frac{-2\delta\Omega^2}{3} \right) \int_0^t dt_1 \int_0^{t_1} dt_2 \varphi(t_1 - t_2). \quad (13)$$

The curved dotted line can hence be thought as the propagator of a fictitious field. A comprehensive presentation of the diagrammatic rules can be found in,

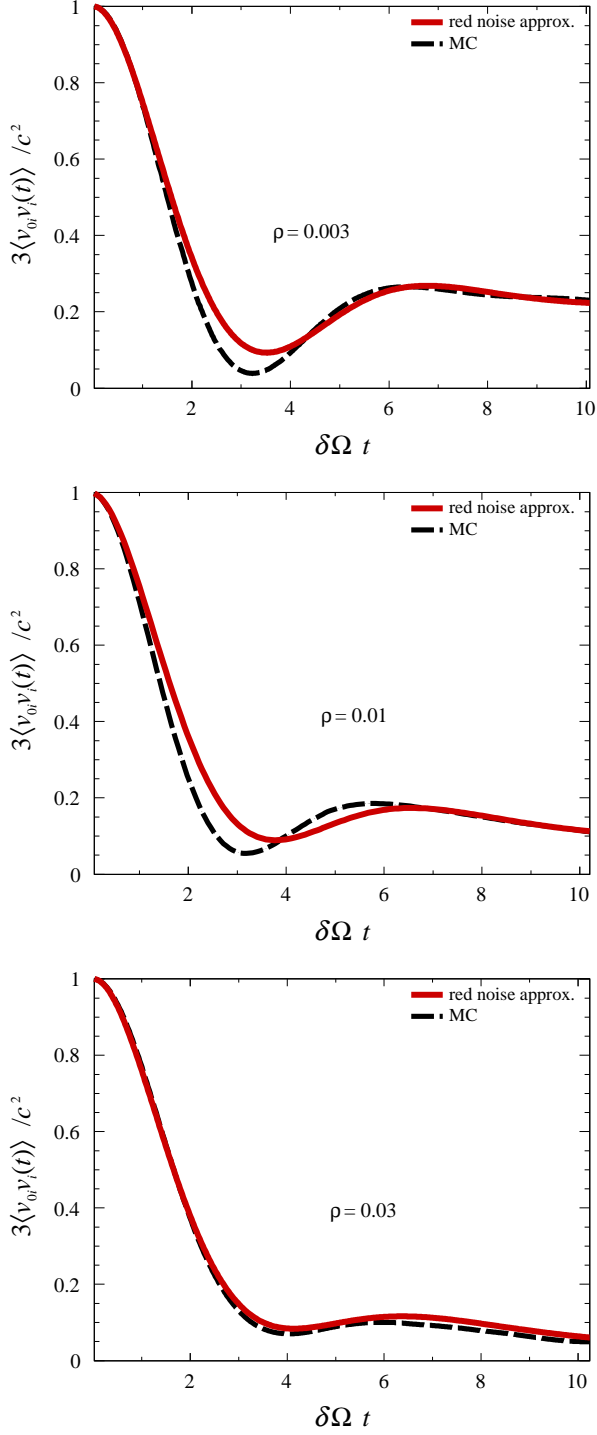


Figure 2. Time dependence of the auto-correlation of the particle velocities expressed in units of $c^2/3$ ($u(t)$ function) for values of rigidities $\rho = 0.003$ (top), $\rho = 0.01$ (middle), and $\rho = 0.03$ (bottom).

transform. Although n must be formally sent to infinity, a truncation to $n \leq 2$ of this partial summation turns out to provide satisfactory results. Such a truncation

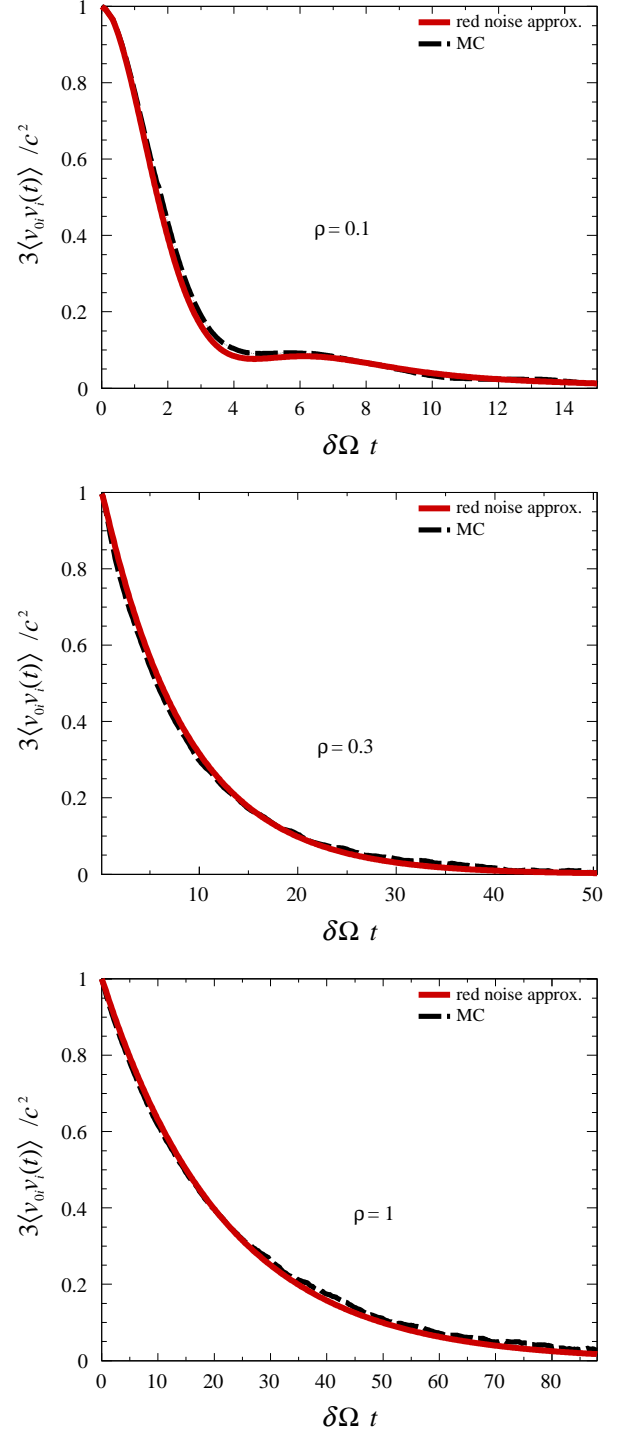


Figure 3. Same as Fig. 2 for values of rigidities $\rho = 0.1$ (top), $\rho = 0.3$ (middle), and $\rho = 1$ (bottom).

corresponds to approximating equation 23 by

$$\begin{aligned} \text{---} \text{---} &\approx \text{---} + \text{---} \text{---} \text{---} + \\ &\text{---} \text{---} \text{---} \end{aligned} \quad (25)$$

Comparisons of $u^{(2)}(t)$ with the Monte-Carlo results are shown in Fig. 2 and 3 for several values of rigidities. For $\rho \leq 0.01$, a range of rigidities such that the Larmor radius of the particles is smaller than the smallest wavelengths of the turbulence, the main features of the time evolution of $u(t)$ are captured by the various approximations leading to $u^{(2)}(t)$ but a good agreement cannot be claimed. By contrast, for values of $\rho > 0.01$ such that the Larmor radius is in gyro-resonance with wavelengths of the turbulence or larger than the size of the largest eddies, agreement between the red-noise approximation and the Monte-Carlo is observed. In particular, the non-exponential fall-off that holds in the gyro-resonant regime, probed in several numerical studies (Candia & Roulet 2004; Fraschetti & Giacalone 2012), is reproduced. As ρ is increasing, the range over which $u^{(2)}(t)$ is significantly non-zero (scattering time scale) increases from several to very many multiples of 2π in terms of $\delta\Omega t$. This illustrates that in the high energy regime, the scattering time scale gets much larger than the correlation one; an exponential fall-off is then recovered (Plotnikov et al. 2011).

4. HINTS IN PRESENCE OF A MEAN FIELD

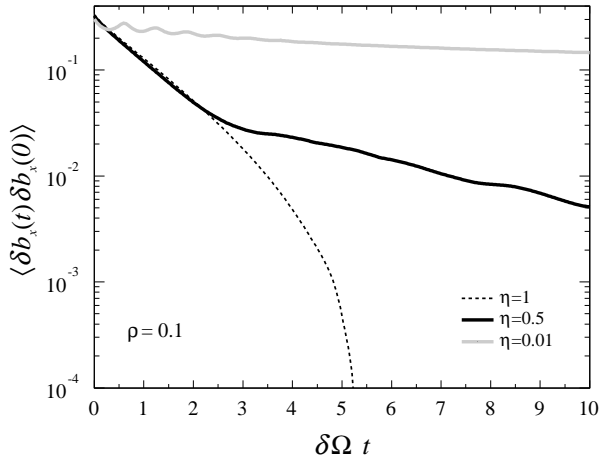


Figure 4. Time dependence of the expectation value of $\langle \delta b_x(t) \delta b_x(0) \rangle$ for three different turbulence levels and $\rho = 0.1$.

Although the case of a purely turbulent magnetic field is relevant in some astrophysical contexts, most cases of interest must deal with intermediate or low levels of turbulence. The numerous Monte-Carlo studies exploring the (η, ρ) parameter space have revealed non-trivial behaviors, in particular for the running perpendicular and anti-symmetric coefficients. Adapting the formalism presented in Section 3 to the case of a mean field on top of a turbulence turns out to be non-trivial without introducing several free parameters. In the following, only a few hints illustrating the required additional ingredients are given.

One key ingredient is the modeling of the 2-pt correlation function of the magnetic field experienced by the particles between two successive times. The presence of a mean field modifies the picture presented in Section 3.1 in a way that the red-noise approximation is no longer valid. This is illustrated in Fig. 4, where the xx -component of the $\langle \delta b_i(t) \delta b_j(0) \rangle$ function is shown for $\rho = 0.1$ (gyro-resonant regime) and for three levels of turbulence, namely $\eta = 1$, $\eta = 0.5$, and $\eta = 0.01$. In the cases $\eta < 1$, the mean field is oriented in the z direction, perpendicular to the initial directions of the test particles. The mean field is observed to introduce a longer time-scale memory on top of that stemming from the turbulence, the intensity of which relative to that of the turbulence is increasing with decreasing values of η .

The longer time scale memory is expected to induce oscillations in the velocity auto-correlation function on a shorter time scale compared to that of the mean field-induced oscillations, which are driven by the Larmor frequency of the particles in spiral motion around the mean field. This effect has been observed in Monte-Carlo simulations to give rise to a sub-diffusive regime for the perpendicular and anti-symmetric running coefficients prior to reaching the plateau of the diffusion regime (e.g. Candia & Roulet 2004; Casse et al. 2001; Fraschetti & Giacalone 2012). A comprehensive characterization of the $\langle \delta b_i(t) \delta b_j(0) \rangle$ function is however beyond the scope of this study and is left for a future one.

5. DISCUSSION

A derivation of the diffusion coefficient describing the propagation of cosmic rays in a 3D isotropic turbulence has been presented, extending the pioneering work of Plotnikov et al. (2011) to the case of a range of rigidities gyro-resonant with the power spectrum of the turbulence. The derivation relies on a single time parameter related to the turbulence correlation time that describes in an economic way the 2-pt correlation function of the magnetic field experienced by the particles between two successive times as a red-noise process. Technically, such

a red-noise approximation makes possible a partial resummation of the Dyson series that solves the equation of motion for the particle velocities.

The red-noise approximation has shown to be a valid one for both the gyro-resonant and the high-rigidity regimes. However, it fails to describe the regime in which particles have a Larmor radius smaller than the smallest scale of the turbulence. In such cases, a modeling of the $\langle \delta b_i(t) \delta b_j(0) \rangle$ functions beyond an exponential fall-off together with a summation of the Dyson series beyond the approximations used in Section 3.2 is required.

More generally, better modelings of the $\langle \delta b_i(t) \delta b_j(0) \rangle$ functions are necessary in the case of the presence of a

mean field. The kind of formalism presented in this study could then be used to infer the various dependencies of the three coefficients in equation 1 in the whole parameter space (ρ, η) .

ACKNOWLEDGMENTS

I thank Haris Lyberis for his numerous works at an earlier stage of this study, and Carola Dobrigkeit for her careful reading of the paper.

APPENDIX

A. NON-CONVERGENT TRUNCATION OF THE DYSON SERIES

In the same spirit as the examples presented in Kraichnan (1961), the calculation carried out in this appendix is an illustration of the benefit to restrict the summation of the Dyson series to tractable classes of terms to all orders such as equation 23.

The diagrams, denoted as $f_n^k(t)$, are classified below accordingly to two numbers, $n = 2m$ and $k = 2\ell$, with n the total number of points and k the number of crossed or nested points. Diagrams with a different topology but sharing the same k and n numbers have equal contributions. For instance, the following nested and crossed diagrams are equal:

$$f_4^2(t) = \text{---} \overbrace{\text{---}}^{\text{---}} \text{---} = \text{---} \overbrace{\text{---}}^{\text{---}} \text{---}, \quad (\text{A1})$$

$$f_6^4(t) = \text{---} \overbrace{\text{---}}^{\text{---}} \text{---} = \text{---} \overbrace{\text{---}}^{\text{---}} \text{---} = \text{---} \overbrace{\text{---}}^{\text{---}} \text{---} = \text{---} \overbrace{\text{---}}^{\text{---}} \text{---}. \quad (\text{A2})$$

We remind that dashed lines indicate integrations over the ordered times crossing the continuous line. For instance,

$$\text{---} \overbrace{\text{---}}^{\text{---}} \text{---} = \left(\frac{-2\delta\Omega^2}{3} \right)^3 \int_0^t dt_1 \int_0^{t_1} dt_2 \int_0^{t_2} dt_3 \int_0^{t_3} dt_4 \int_0^{t_4} dt_5 \int_0^{t_5} dt_6 \varphi(t_1 - t_3) \varphi(t_2 - t_5) \varphi(t_4 - t_6). \quad (\text{A3})$$

An attempt to carry out a summation of all terms up to some order k_{\max} can be made by weighting all $f_{2m}^{2\ell}$ functions by the combinatorics that determines their number of occurrence. For $k = 0$, one is left with the series of unconnected diagrams, each of them with weight 1; this is the Bourret propagator. For $k = 2$, there are $2(m-1)$ ways to insert one nested or crossed diagram among $2m-4$ unconnected ones. For $k = 4$, a minimal number of $n = 6$ points is required. There are four crossed/nested ways to join the points that give rise to the same contribution (equation A2), and, for $m > 2$, there are $\binom{m-2}{m-3}$ distinct ways to insert any of these diagrams among $n-6$ points joined with unconnected diagrams. In addition, starting from $n = 8$ points, there are four possibilities to connect any of the diagrams of equation A1 into $n = 8$ points, and there are $\binom{m-2}{2}$ ways to insert them among $n-8$ points. This leads to the contribution

$$u(t; k=4) = \sum_m \left[4 \binom{m-2}{m-3} f_{6,m>2}^4(t) + 4 \binom{m-2}{2} f_{8,m>3}^4(t) \right]. \quad (\text{A4})$$

For $k = 6$, a minimal number of $n = 6$ points is required. There are six crossed/nested ways to join the points that give rise to the same contribution, $f_6^6(t)$. Contributions to $f_n^6(t)$ can also arise with $n = 8$ (eight different diagrams), with $n = 10$ by connecting $f_6^4(t)$ and $f_4^2(t)$ with any number of unconnected diagrams (sixteen different diagrams denoted as $f_{10}^{4+2}(t)$), and with $n = 12$ by connecting three $f_6^4(t)$ diagrams (eight different diagrams). The associated combinatorics reads as

$$u(t; k = 6) = \sum_m \left[6 \binom{m-2}{m-3} f_{6,m>2}^6(t) + 8 \binom{m-3}{m-4} f_{8,m>3}^6(t) + 16 \binom{m-3}{m-5} f_{10,m>4}^{4+2}(t) + 8 \binom{m-3}{3} f_{12,m>5}^{2+2+2}(t) \right]. \quad (\text{A5})$$

The reasoning can be repeated for higher values of k , although the increasing number of terms gets quickly non-tractable. For $k = 8$, the contribution reads as

$$u(t; k = 8) = \sum_m \left[24 \binom{m-3}{m-4} f_{8,m>3}^8(t) + 16 \binom{m-4}{m-5} f_{10,m>4}^8(t) + 24 \binom{m-3}{m-5} f_{10,m>4}^{6+2}(t) + 16 \binom{m-4}{m-6} f_{12,m>5}^{4+4}(t) \right. \\ \left. + 32 \binom{m-4}{m-6} f_{12,m>5}^{6+2}(t) + 48 \binom{m-4}{m-7} f_{14,m>6}^{4+2+2}(t) + 16 \binom{m-4}{4} f_{16,m>7}^{2+2+2+2}(t) \right], \quad (\text{A6})$$

and so on and so forth.

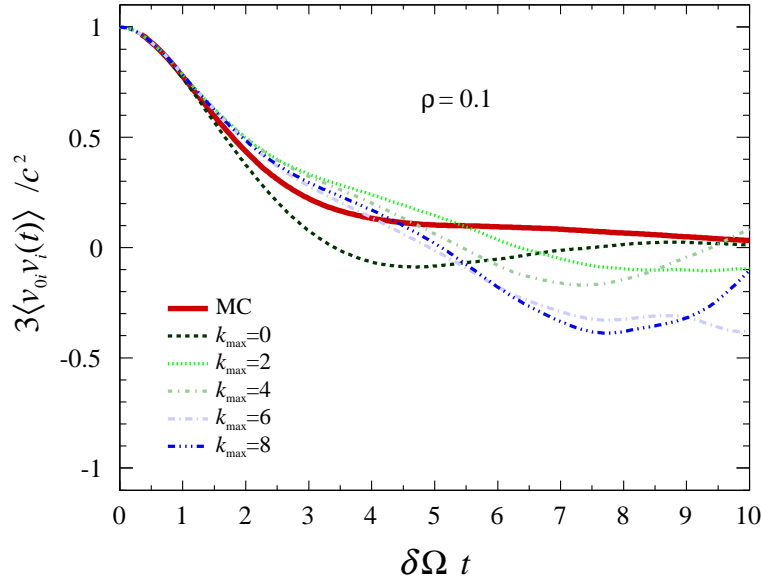


Figure 5. $u(t; k_{\max})$ for several values of truncation k_{\max} .

Comparisons between $u(t; k_{\max}) = \sum_{k=0}^{k_{\max}} u(t; k)$ and $u^{(2)}(t)$ obtained from the Kraichnan propagator are shown in Fig. 5. It can be seen that the truncation to any value of k_{\max} as high as 8 fails to produce a physical solution for $t \gtrsim 2/(3\delta\Omega^2\tau)$. This clearly illustrates the benefit of using the Kraichnan propagator.

REFERENCES

- | | |
|---|---|
| <p>Batchelor, G. K. 1970, The theory of homogeneous turbulence (Cambridge University Press)</p> <p>Bhatnagar, P. L., Gross, E. P., & Krook, M. 1954, Phys. Rev., 94, 511, doi: 10.1103/PhysRev.94.511</p> <p>Bourret, R. C. 1962, Il Nuovo Cimento, XXVI, 3833, doi: doi.org/10.1007/BF02754339</p> | <p>Candia, J., & Roulet, E. 2004, JCAP, 10, 007, doi: 10.1088/1475-7516/2004/10/007</p> <p>Casse, F., Lemoine, M., & Pelletier, G. 2001, Phys. Rev. D, 65, 023002, doi: 10.1103/PhysRevD.65.023002</p> <p>Corrsin, S. 1959, Advances in Geophysics, Atmospheric Diffusion and Air Pollution, Vol. 6 (New York: Academic)</p> |
|---|---|

- Fatuzzo, M., & Melia, F. 2014, *Astrophys. J.*, 784, 131, doi: [10.1088/0004-637X/784/2/131](https://doi.org/10.1088/0004-637X/784/2/131)
- Fraschetti, F., & Giacalone, J. 2012, *Astrophys. J.*, 755, 114, doi: [10.1088/0004-637X/755/2/114](https://doi.org/10.1088/0004-637X/755/2/114)
- Frisch, U. 1966, *Annales d'Astrophysique*, 29, 645
- Giacalone, J., & Jokipii, J. R. 1999, *ApJ*, 520, 204, doi: [10.1086/307452](https://doi.org/10.1086/307452)
- Hauff, T., Jenko, F., Shalchi, A., & Schlickeiser, R. 2010, *ApJ*, 711, 997, doi: [10.1088/0004-637X/711/2/997](https://doi.org/10.1088/0004-637X/711/2/997)
- Jokipii, J. R. 1966, *ApJ*, 146, 480, doi: [10.1086/148912](https://doi.org/10.1086/148912)
- . 1972, *ApJ*, 172, 319, doi: [10.1086/151349](https://doi.org/10.1086/151349)
- . 1973, *ApJ*, 183, 1029, doi: [10.1086/152289](https://doi.org/10.1086/152289)
- Jones, F. C. 1990, *ApJ*, 361, 162, doi: [10.1086/169179](https://doi.org/10.1086/169179)
- Kraichnan, R. H. 1961, *Journal of Mathematical Physics*, 2, 124, doi: <https://doi.org/10.1063/1.1724206>
- Kubo, R. 1957, *J. Phys. Soc. Jap.*, 12, 570, doi: [10.1143/JPSJ.12.570](https://doi.org/10.1143/JPSJ.12.570)
- Plotnikov, I., Pelletier, G., & Lemoine, M. 2011, *Astron. Astrophys.*, 532, A68, doi: [10.1051/0004-6361/201117182](https://doi.org/10.1051/0004-6361/201117182)
- Reichherzer, P., Becker Tjus, J., Zweibel, E. G., Merten, L., & Pueschel, M. J. 2020, *Mon. Not. Roy. Astron. Soc.*, 498, 5051, doi: [10.1093/mnras/staa2533](https://doi.org/10.1093/mnras/staa2533)
- Reichherzer, P., Merten, L., Dörner, J., et al. 2021. <https://arxiv.org/abs/2104.13093>
- Snodin, A. P., Shukurov, A., Sarson, G. R., Bushby, P. J., & Rodrigues, L. F. S. 2016, *Mon. Not. Roy. Astron. Soc.*, 457, 3975, doi: [10.1093/mnras/stw217](https://doi.org/10.1093/mnras/stw217)
- Thomson, J. J., & Benford, G. 1973, *Journal of Mathematical Physics*, 14, 531, doi: [10.1063/1.1666349](https://doi.org/10.1063/1.1666349)